DEU FMD 26(77) (2024) 341-349

Dokuz Eylül Üniversitesi Mühendislik Fakültesi Fen ve Mühendislik Dergisi
Dokuz Eylul University Faculty of Engineering Journal of Science and Engineering
Elektronik/Online ISSN: 2547-958X

RESEARCH ARTICLE / ARAŞTIRMA MAKALESI

Adjustable Friction Force of Elastic Post via Regulating Internal Cavity Pressure

Kavite Boşluk Basıncını Düzenleyerek Elastik Çubuğun Ayarlanabilir Sürtünme Kuvveti

Turgay Eray

[1]Department of Mechanical Engineering, Faculty of Engineering, Aydın Adnan Menderes University, Efeler, Aydın, TÜRKİYE
Corresponding Author / Sorumlu Yazar *: turgay.eray@adu.edu.tr

Abstract

The objective of this study is to investigate and obtain an adjustable friction force between an elastic polymeric post with cavity and a rigid, smooth, flat surface. Elastic cylindrical posts made of polymers are generally used as surface texturing components. In this study, the friction force of the elastic cylindrical posts with a flat tip in contact with a smooth and rigid surface was adjusted by a pneumatic-based actuation system. Finite-element based simulation was performed to adjust the friction force of the cylindrical posts by pressurizing the inner cavity of the posts. The frictional contact between the elastic posts and the counter rigid surface was modeled using the Amontons-Coulomb friction law, neglecting the adhesive contribution. The friction force amplitude was calculated with different cavity dimensions of the elastic posts and different cavity pressure values. The results show that the presence of an internal cavity reduces the friction force, and the cavity diameter has more influence on the reduction of the friction force than the cavity height. In conclusion, regulating the cavity pressure was shown to be an effective method of adjusting the friction force.

Keywords: *Friction, Adjustable Friction, Elastic Post, Pressurized Cavity, Bending Rigidity*

Öz

Bu çalışmanın amacı, polimerik malzemeden yapılmış kavite içeren elastik bir çubuk ile sert, pürüzsüz, düz bir yüzey arasında ayarlanabilir bir sürtünme kuvvetinin araştırılması ve elde edilmesidir. Polimerlerden yapılan elastik silindirik çubuklar genellikle yüzey desenleme bileşeni olarak kullanılır. Bu çalışmada, düz ve rijit bir yüzeyle temas halinde olan düz uçlu elastik silindirik çubukların sürtünme kuvveti pnömatik tabanlı eyleyici sistemi ile ayarlanmıştır. Silindirik çubukların sürtünme kuvvetini çubukların iç kaviteye basınç uygulayarak ayarlamak için sonlu elemanlar tabanlı simülasyon gerçekleştirilmiştir. Elastik çubuklar ile karşıt rijit yüzey arasındaki sürtünme kuvveti, adeziv katkısı ihmal edilerek Amontons-Coulomb Sürtünme Kanunu kullanılarak modellenmiştir. Sürtünme kuvvet genliği, elastik çubukların farklı kavite boyutları ve farklı kavite basınç değerleri ile hesaplanmıştır. Bulgular; kaviteye sahip olmanın sürtünme kuvvetini azalttığını, kavite çapının sürtünme kuvvetinin azalması üzerinde kavite uzunluğundan daha fazla etkiye sahip olduğunu göstermektedir. Sonuç olarak, kavite içindeki basıncı düzenlemenin sürtünme kuvvetini ayarlamak için etkili bir yöntem olduğu gösterilmiştir.

Anahtar Kelimeler: *Sürtünme, Ayarlanabilir Sürtünme, Elastik Çubuk, Basınçlı Kavite, Eğilme Rijitliği*

1. Introduction

Adjustable contact forces have been in favor for engineering applications, where the contact forces can be altered by modifying the contacting surfaces. One example of the surface modification is surface texturing [1–7]. Depending on the material of the surfaces, this method can be achieved by coating, molding, classical machining, laser fabrication, and soft lithography techniques. For soft contact with relatively low Young's modulus (~3 MPa), elastic posts are the most used structural component to texture the surfaces, where changing the structural parameters of elastic posts leads to changing the contact forces [8-12]. By using elastic posts mainly made of polymeric material such as Polydimethylsiloxane, contact parameters (contact pressure, contact forces, contact area etc.) are distributed to these elastic posts. This effect is called contact splitting [13]. Therefore, different structural parameters of elastic posts yield different contact parameters. Thus, playing with the elastic posts physical and geometrical parameters such as dimension, material etc. results in an adjustable contact condition. This can be called a passive tuning strategy to adjust the contact parameters. However, it is important to emphasize that after the elastic posts are manufactured, it would be very difficult to modify the structural and geometrical parameters of the posts to adjust the contact parameters without external actuation. Furthermore, it is necessary to provide a possible external actuation mechanism to be able to alter the contact parameters using elastic posts. In this case, the elastic posts should be designed and manufactured in accordance with the external actuation system.

The friction force of elastic posts in contact with a smooth rigid body depends on the bending rigidity of the posts. In addition, it has been shown that friction force amplitude can be approximately calculated by using bending and axial rigidity of the posts based on the assumption that the contact is partitioned

DOI:10.21205/deufmd.2024267719

Atıf şekli / How to cite:
Eray,T. (2024). Adjustable Friction Force of Elastic Post via Regulating Internal Cavity Pressure. DEUFMD, 26(77), 341-349.

Geliş Tarihi / Received: 01.04.2023
Kabul Tarihi / Accepted: 11.12.2023

into stiff components [14–16]. Furthermore, the friction force of elastic posts in contact with a smooth rigid body can also be altered by actively changing the dimensions of the posts (effective height and orientation of the post tip with respect to the friction direction) [17]. Here, changing the effective height and tip orientation modifies the bending rigidity of the posts. Therefore, modifying the bending rigidity of elastic posts would lead to an adjustable friction force between the elastic posts and smooth rigid body. The bending rigidity of mechanical systems can be modified by using two main methods: 1- Playing with the modulus of elasticity by making a composite material with two different materials [18–20]; 2- External actuation mechanism such as pneumatic [21], which is a simple way to modify the bending rigidity of the elastic posts. In addition, to provide pneumatic actuation, the elastic component must have some kind of internal structure [21–25], where air could be supplied. Related previous works have not investigated the effect of the internal structure on the friction of elastic posts. Therefore, it is necessary to investigate the effect of the internal structure dimension on the friction force of elastic posts in contact with a smooth rigid body.

In this study, the friction force of elastic posts in contact with a smooth rigid body was investigated by using a finite-element based engineering program. The elastic posts have an internal cavity to which pressurized air could be supplied, where the effect of internal cavity dimension and cavity pressure on the friction force amplitude was investigated. In section two, materials and method are described in detail. Section three presents the results and discussion. Finally, in section four, the conclusion is given.

2. Materials and Methods

The frictional dynamics between an elastic cylindrical post and a rigid smooth and flat surface was simulated in a finite-element based engineering program (COMSOL Multiphysics 5.3a). A two-dimensional (2D) structural model of the posts was constructed in the software. The friction law governing the frictional motion between the elastic posts and the rigid counter surface was modelled by using Amontons-Coulomb friction law with a single coefficient. In another study, this friction model between an elastic post and a rigid, flat body with a single coefficient were shown to be in agreement with the experimental results in [14,20]. The same procedure was adopted in this study.

2.1. Structure of the posts and simulation parameters

In the simulations, the elastic posts have same diameter and height. Different diameters and different lengths are considered for the internal cavity in the posts. The friction force between the posts and the rigid counter surface was investigated under different internal cavity pressures by keeping the diameter and height of the inner cavity constant. The simulation sets formed by varying the constructional parameters of the posts and the simulation conditions are given in Table 1 and shown in Figure 1. Here, D is post diameter, H is post height, d is cavity diameter, and h is layer thickness over the cavity.

Table 1. The simulation sets and structural parameters of the posts used in the simulation sets.

Sets	*R:D/2*	*H*	*d/R*	*h*	*P*
Set-h (Cavity height effect)	4 mm	24 mm	1	0.2:0.2:4 mm	0 bar
Set-d (Cavity diameter effect)	4 mm	24 mm	(0.2:0.2:1)	1 mm	0 bar
Set-P (Cavity pressure effect)	4 mm	24 mm	1	2 mm	0.5:0.1:1 bar

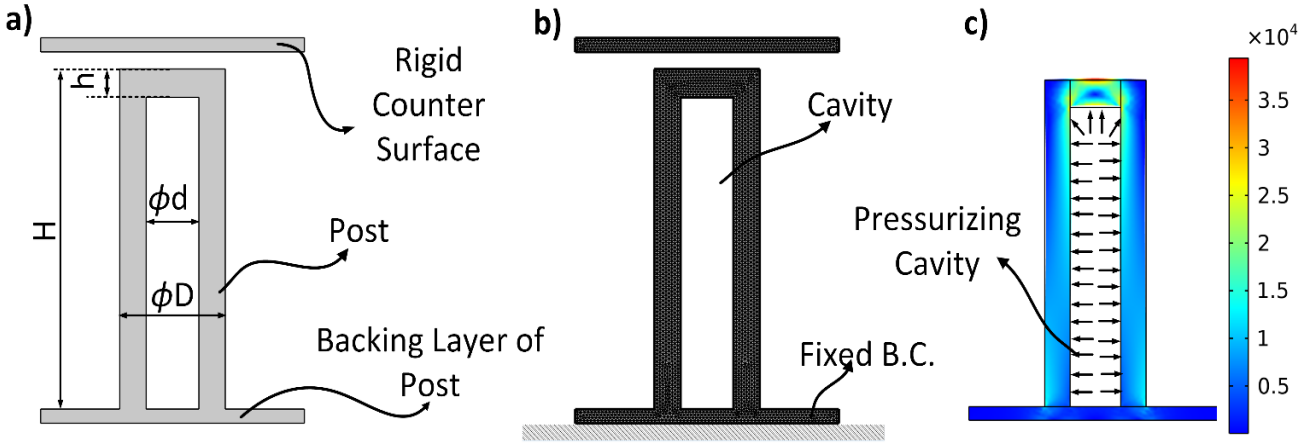

Figure 1. a) Design parameters of the elastic posts, b) Structure of the mesh in the simulations, c) Pressurized state and the resulting von Mises stress in Pa

2.1.1. Physical parameters in the simulations and the simulation procedure

The elastic material of the posts is Polymethylsiloxane (PDMS), which has a Young Modulus of 2 MPa. The Young's Modulus of the rigid counter surface is chosen to be 70 GPa. The viscoelastic effects of the PDMS and the counter surface are neglected. The friction model between the post and the counter surface is defined by a single friction coefficient, which is 0.3. By keeping this value constant, only the structural effects of the posts and the

cavity pressure effect on the friction force were examined. A typical time-contact force result and the simulation stages on the finite-element based engineering software are depicted in Figure 2.

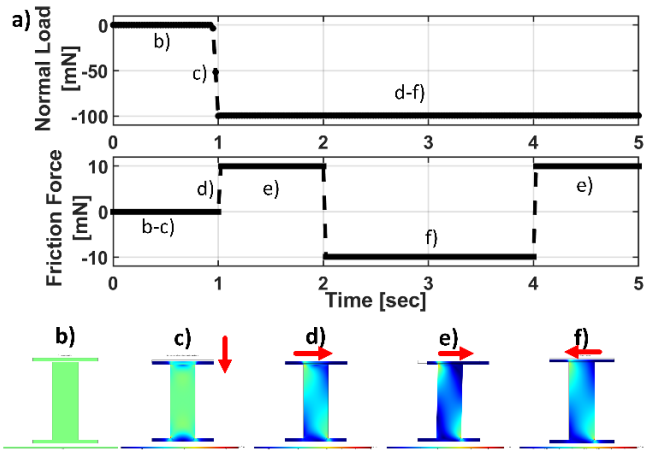

Figure 2. Typical simulation result: a) Time-normal and time-friction force results are presented, revealing the stages of frictional motion. During these stages, the counter surface moves in the direction indicated by the red arrow. b) Initially, there is no contact between the post and the counter surface. c) Subsequently, full contact is established under a certain preload value. d) At this point, the counter surface is laterally displaced, and the post and the counter surface are sticking. e) Once the friction force reaches the threshold value [26], the post transitions to full-sliding motion. f) Finally, the counter surface is moved in the opposite direction to obtain the friction force-displacement loop

2.1.2. Mesh convergency study

The Comsol Multiphysics software offers different predefined mesh sizes from extremely coarse to extremely fine. Each predefined mesh automatically generates the mesh model of the structural components, resulting in a different number of boundary and domain elements, and degrees of freedom. In our study, six different predefined mesh sizes are selected and compared with the results of the extremely fine mesh size for friction force magnitudes in the sliding regime (e-f in Figure 2). The relative error is defined as Err=1000*(E.F-M.S)/E.F. The results are shown in Table 2. From the results, the most accurate solution is the extremely fine mesh study. However, due to the increased number of degrees of freedom and the closeness of the results to the extremely fine mesh, the extra fine mesh is selected for further simulations. For the selected mesh, the relative error is around %0.02.

2.1.3. Simulation procedure for the frictional motion without pressurizing cavity of the posts

The stages of the frictional motion between the post and the counter surface for the frictional motion given in the sets (Set-h & Set-d) are as follows:

- ✓ There is no contact between the opposite surface and the post as depicted in Figure 2(b).
- ✓ The post is compressed by applying uniaxial to the counter surface. Then, the full contact is obtained between the post and the counter surface with a desired preload value as shown in Figure 2(c). The post is fixed from its backing layer. Here, the preload value between the post and the counter surface is selected as Fp=0.10, 0.25, 0.50, 0.75, 1.00 N.
- ✓ After the desired preload value is achieved between the counter surface and the post, the counter surface moves in the lateral direction, and hence friction is attained between the post and the counter surface as depicted in Figure 2(d).
- ✓ When the friction force between the post and the counter surface reaches the threshold value [26], the post goes into full-sliding motion. The normal and friction forces remain constant during the full sliding motion of the post as shown in Figure 2(e). The friction force is at its maximum value at this stage, and this value is considered in the next sections.
- ✓ The friction force-displacement loop is obtained by moving the counter surface in the opposite direction as given in Figure 2(f).

Table 2. Mesh converge study for the constructed simulation model.

Predefined Mesh Sizes (M.S.)	Coarse	Normal	Fine	Finer	Extra Fine	Extremely Fine (E.F)
Domain Element Number	144	244	352	732	2254	8594
Boundary Element Number	88	102	112	156	284	566
Number of degrees of freedom	781	1249	1713	3357	9785	35889
Friction Force [mN]	9.9699	9.9684	9.9539	9.9524	9.9300	9.9271
Error (%) in Friction Force	-‰4.360	-‰4.311	-‰2.700	-‰2.549	-‰0.292	-

2.1.4. Simulation procedure for the frictional motion with pressurized cavity of the posts

The effect of the cavity pressure on the friction force was investigated in two configurations. In the first configuration, there is no contact between the post and the counter surface. The cavity of the posts is pressurized prior the contact. In this configuration, the normal force between the post and the counter surface can be obtained at the desired value. This gives a friction force result with pressurized cavity in pre-contact configuration. In the second configuration, the posts and the counter surface are in full contact. Then, the cavity of the post is pressurized. However, with the cavity pressurized, the normal force may differ from the desired preload value. This configuration is also divided into two parts. The first one is to obtain the friction force with the pressure values specified in Table 1, and the second is to attain the friction force by applying pressure to cavity for the desired normal load. In the first configuration, the post and the counter surface are not in contact. The post is pressurized prior to contact. The simulation protocol is as follows:

- ✓ There is no contact between the post and the counter surface. At this stage, the cavity of the post is pressurized as depicted in Figure 3(c-ii).
- ✓ The post is compressed by the counter surface until the desired preload value is achieved between the post and the counter surface. Meanwhile, the pressure in the post cavity is kept constant as shown in Figure 3(c-iii).
- ✓ As shown in Figure 3(c-ii), the desired preload value is attained. The counter surface is moved laterally to obtain friction force. A typical time-normal and friction force, time-cavity pressure results are shown in Figure 3.

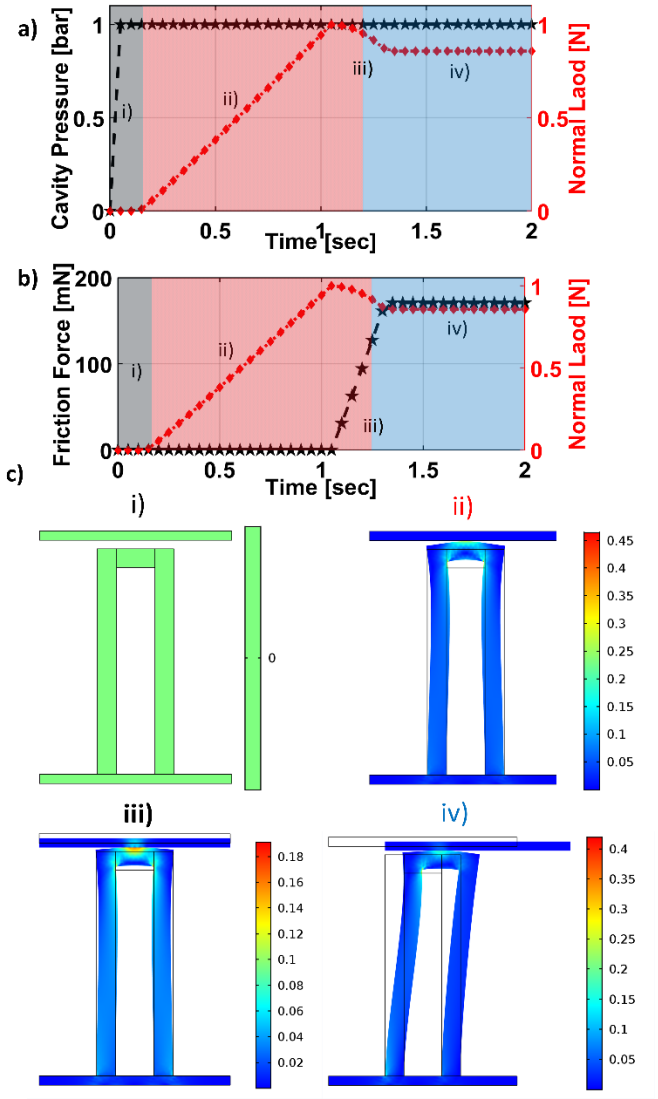

Figure 3. Typical results with the pressurized cavity prior to contact between the post and the counter surface; a) Cavity pressure, normal load, b) Friction force-normal load; where the black line represents the cavity pressure and the friction force, the red line represents the normal force value. The preload value is 1 N, and the cavity pressure value is 1 bar. c) The steps in the simulations; i) There is no contact between the post and the counter surface, ii) The cavity of the post is pressurized to a desired value, iii) The post is compressed by the counter surface until the normal force reaches the desired preload value, iv) The friction force is obtained by moving the counter surface in the lateral direction. The legend shows the von Mises stress in MPa

In the second configuration, there is a contact between the post and the counter surface, the contact force is approximately 0 N. The cavity of the post is pressurized and as in the other stages, when the desired pressure value is reached, the counter surface moves in the lateral direction. Hence, the friction force is obtained. There are two key points to mention. These are 1) the deviation of the normal load value from the desired preload value due to the desired pressurized cavity, 2) the adjustment of the cavity pressure to obtain the desired preload value. The typical result and the phases of the simulation are given in Figure 4. The simulation procedure is as follows:

- ✓ The counter surface is in contact with the post. The normal force is approximately 0 N.
- ✓ By restricting the movement of the counter surface in direction parallel to the cavity pressurized direction, it is ensured that there is a contact between the counter surface and the post at every simulation stages.
- ✓ The cavity of the post is pressurized. Because of the restricted movement of the counter surface, a normal force is achieved between the post and the counter surface as depicted in Figure 4, 1st Phase.
- ✓ When the cavity pressure reaches the desired maximum pressure value, the maximum normal force value is obtained between the counter surface and the post, End of 1st Phase. After this step, the counter surface moves laterally. Hence, frictional motion is obtained, 2nd Phase. During this motion, the cavity pressure is kept constant.

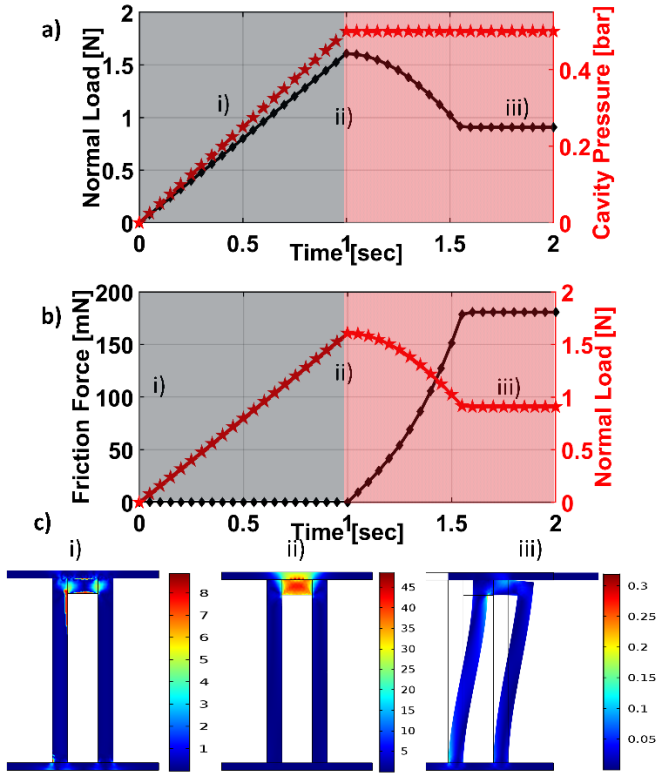

Figure 4. The effect of cavity pressurization on the friction force when the post is in contact with the counter surface. a) Typical normal load-pressure-time and b) friction force-normal load-time results and c) the phases in the simulation. i) The cavity of the post is pressurized and at this time, the normal load between the post and the counter surface increases, ii) The maximum pressure value is reached, and the maximum normal load is obtained. iii) The friction force is obtained by giving lateral motion to the counter surface

3. Results and Discussion

3.1. Effect of layer thickness over the cavity on the friction force

This section presents the results of the effect of the layer thickness over the post cavity on the friction force amplitude are given. The friction force amplitudes were obtained according to five different preload force values (Fp: 0.10, 0.25, 0.50, 0.75 and 1.00 N). The friction force results were normalized with respect to the results of the homogenous post (post without cavity). The results are given in Figure 5.

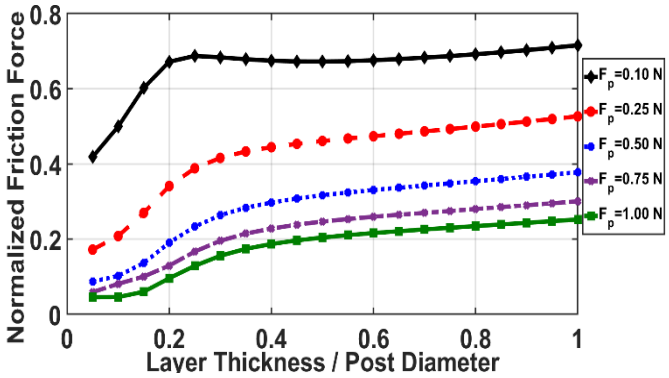

Figure 5. The effect of thickness of the layer on the normalized friction force amplitude obtained under five different preload values (0.1, 0.25, 0.5, 0.75 and 1 N)

As the diameter of the post cavity remains constant and the thickness of the layer over the cavity increases, the frictional force increases. The characteristic of the increase in friction force is the same for all preload values. The change in friction force is linear up to a layer thickness of 0.2 mm over the cavity. After the 0.2 value, the change in frictional force is different for different preload values. This phenomenon can be explained by the fact that when the layer thickness is thin, it behaves like a thin sheet between the post sides. In this case, the elastic deformation of the post tip changes with the layer thickness. The characteristic of decreasing amount of elastic deformation changes with increasing layer thickness. Thus, the effect of different layer thickness on different change of friction force can be explained in this way. Accordingly, Figure 6 and Figure 7 show the elastic deformation and von Mises stress values of the post with the same thin film layer thickness at different preload values, and at the same preload value (1.00 N) but the post with different thin film layer thickness, respectively. As the layer thickness over the cavity increases, the elastic deformation in the layer changes and the amplitude of the normal force between the post and the counter surface changes accordingly.

Since the friction force amplitude is directly related to the contact area at the contact interface [27], alteration of the contact area with varying thickness of the thin film over the cavity yields different friction force. The normal load is the force exerted by the contact pressure over the contact area. The contact area was approximated using the relationship between the normal load at the contact interface and the maximum contact pressure. The normal force and maximum contact pressure for the post with a film layer thickness of 0.2 mm and the variation of the contact area with the different layer thickness are shown in Figures 8 and 9, respectively.

Although the friction force increased with increasing the layer thickness over the cavity, the friction force value is still lower than that of the homogenous post (post without cavity). This phenomenon can be explained by different bending rigidity of the post in the lateral (shear) direction with different layer thickness. The bending rigidity of posts can be approximated by Hooke's law using the maximum deformation of the post for a given lateral force. In Figure 10, the variation of the bending rigidity of the post with respect to the different layer thickness over the cavity is given by normalizing with respect to the bending rigidity of the homogenous post. The bending rigidity of the post increases as layer thickness increases. The change characteristic of the bending rigidity is the same as the change of the friction force characteristic as shown in Figure 10. The lower friction force of the posts due to the cavity can be related to the decrement of the bending rigidity, since the friction force of the posts is directly related to the bending of the post [14,15].

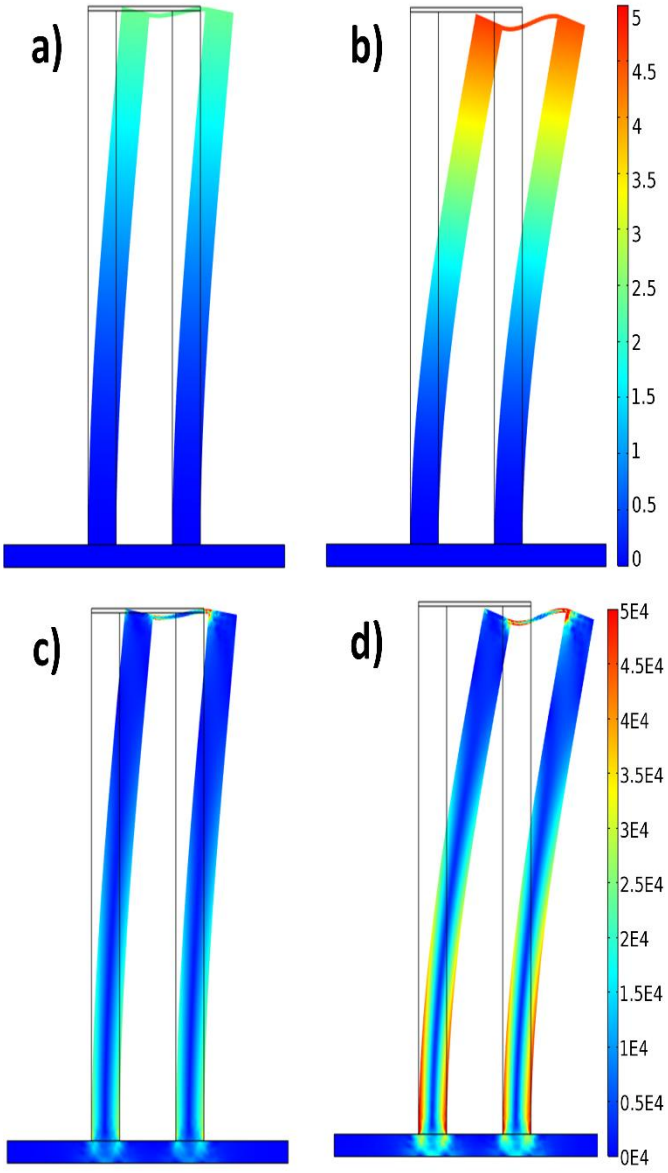

Figure 6. The simulation results, when the cavity diameter of the post is 4 mm and the thickness of the layer over the cavity is 0.2 mm, the elastic deformation and the von Mises stress when the preload value is a-c) 0.10 N, b-d) 1.00 N, respectively. The legend is in mm in a-b) and in Pa in c-d)

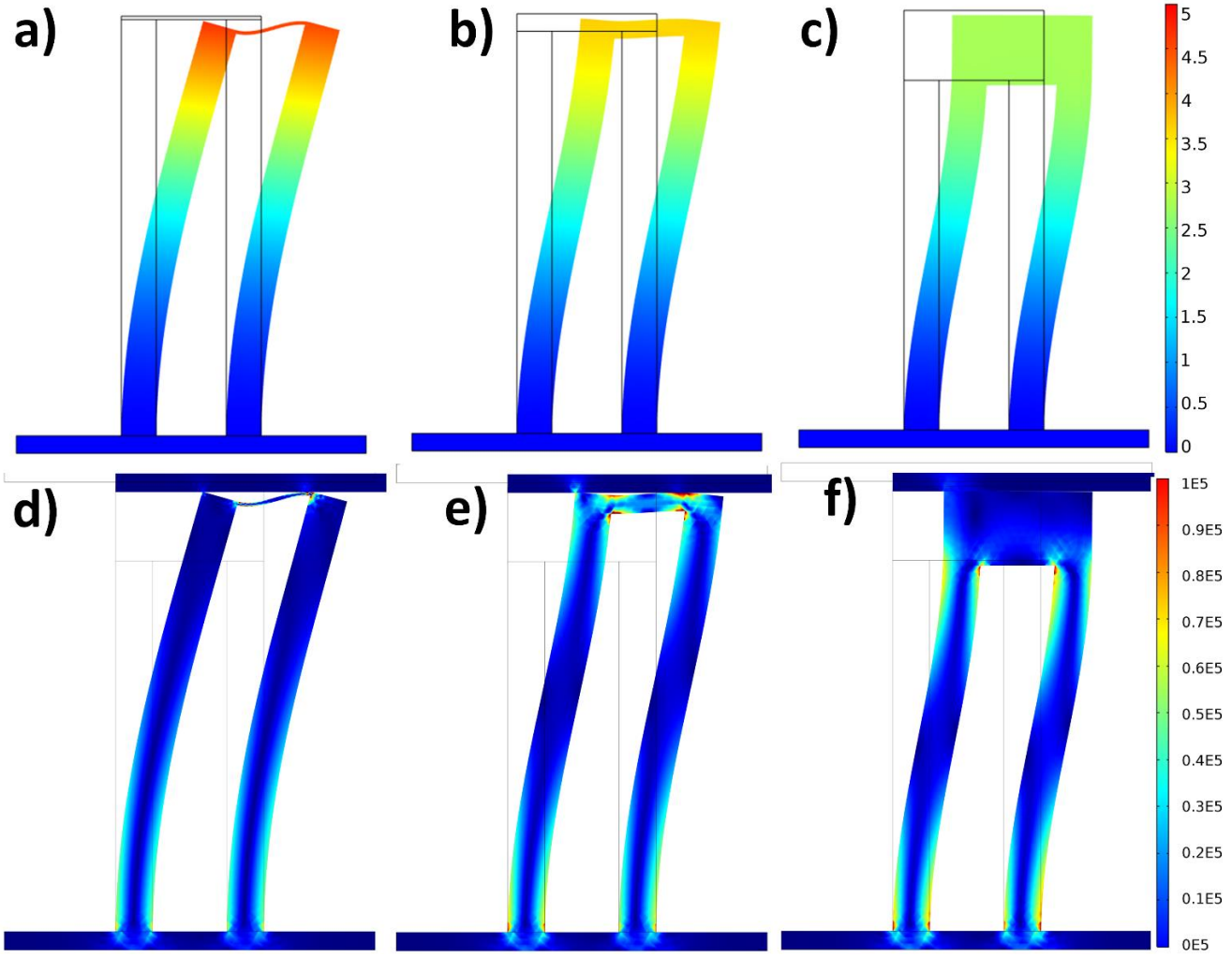

Figure 7. Under the same preload value (1 N), the elastic of deformation and von Mises stress obtained for the posts with the same cavity diameter and different layer thickness values over the cavity, respectively. Layer thickness is a-d) 0.2 mm, b-e) 1 mm, and c-f) 4 mm. The legend is in mm in a-b-c) and in Pa in d-e-f)

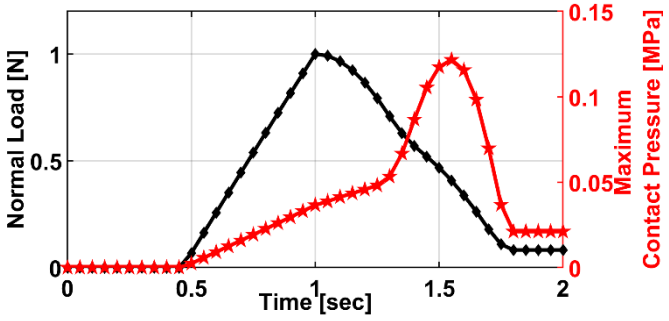

Figure 8. Time evaulation of normal force and contact pressure in the frictional motion of the post with a layer thickness of 0.2 mm and a cavity diameter of 4 mm under a preload of 1.00 N. Here, the black line and the red line represent the normal force and the contact pressure, respectively. The contact area is calculated by dividing the normal load by the maximum contact pressure

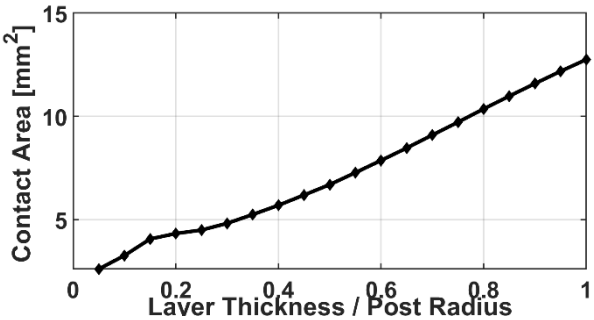

Figure 9. Variation of the approximate contact area with respect to the layer thickness over the cavity in the posts containing different layer thicknesses with a cavity diameter of 4 mm

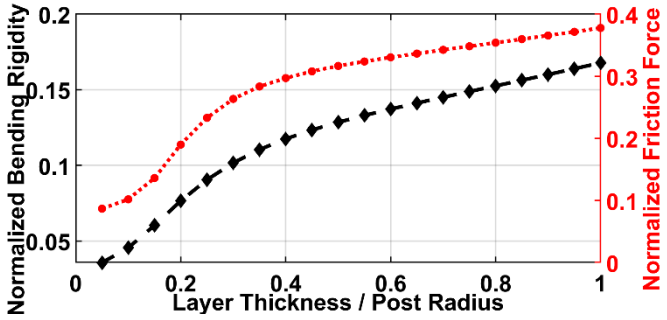

Figure 10. The effect of the layer thickness over the cavity on the bendingrigidity of the post normalized with the bending rigidity of the homogenous post, and the relation between the change of friction force and the change of bending rigidity of the post

3.2. Effect of cavity diameter on the friction Force

The effect of cavity diameter on friction force is achieved by maintaining the layer thickness over the cavity of the posts constant. The amplitude of friction force is normalized with respect to the value of the homogenous post. Figure 11 shows the relationship between the friction force value and cavity diameter. As the cavity diameter increases, the friction force decreases linearly. The maximum decline reaches up to 80%.

The reduction in bending rigidity is caused by the presence of a cavity. Additionally, it should be noted that the diameter of the cavity results in a greater reduction in friction force amplitude compared to the thickness of the layer. This can be explained by the cavity diameter's effect on the posts' bending rigidity at the fourth order, while the layer thickness has a third order effect. Figure 12 illustrates alterations in the friction force and bending rigidity of the post.

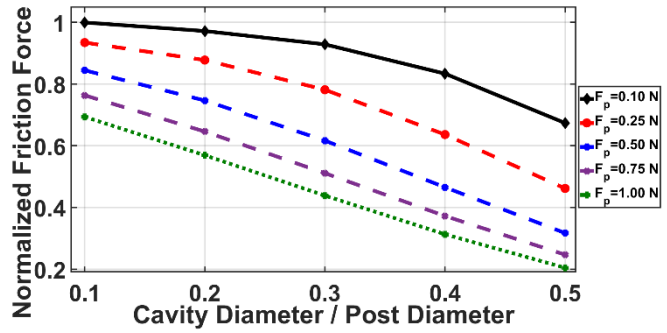

Figure 11. The effect of cavity diameter on the normalized friction force amplitude obtained under five different preload values (0.1, 0.25, 0.5, 0.75 and 1 N)

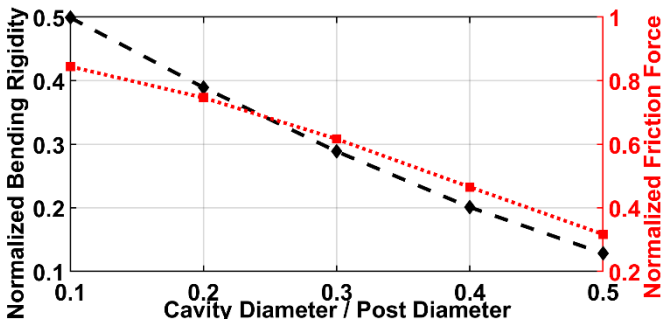

Figure 12. The effect of the cavity diameter on the bending rigidity of the post normalized with the bending rigidity of the homogenous post, and the relation between the change of friction force and the change of bending rigidity of the post

3.3. Effect of cavity pressure on the friction force

In a post with a constant cavity diameter and layer thickness over, the variation of friction force amplitude was investigated by pressurizing the cavity. The friction force amplitude was normalized to the friction force amplitude of the homogenous post. The cavity was pressurized in two instances. 1) The cavity was pressurised after the desired preload value was achieved through static contact. 2) The cavity was pressurised whilst the post and counter surface were in contact with a preload value of approximately 0 N.

3.3.1. Pressurizing the cavity before the contact between the post and the counter surface

The inner cavity of the post is pressurized with amplitudes of 0.5, 0.6, 0.7, 0.8, 0.9 and 1 bar. Figure 13 illustrates the fluctuation of friction force amplitude accompanying the post's cavity pressure. As the cavity pressure amplifies, so does the friction force amplitude; it varies almost linearly with the cavity pressure amplitude. Increasing cavity pressure provokes linear changes in the post's bending rigidity. The bending rigidity of the post is normalized in comparison to the homogenous post, and its variation with pressure is displayed in Figure 14. The linear variation of post bending rigidity with cavity pressure can account for the almost linear variation in friction force amplitude. It is worth noting that there is no contact between the posts and the counter surface when computing the bending rigidity of the posts.

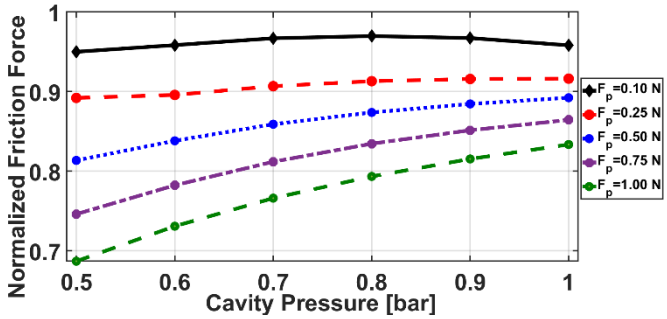

Figure 13. The effect of the post cavity pressure on the friction force amplitude when the cavity was pressurized prior to contact

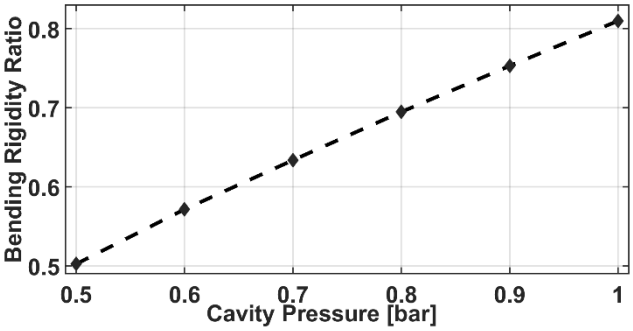

Figure 14. Effect of cavity pressure on the normalized bending rigidity of post

3.3.2. Pressurizing the cavity after the contact between the post and the counter surface

This study examined the effect of cavity pressure amplitude on friction force when the post and counter surface are in contact. To achieve this, the counter surface's movement in the normal direction during cavity pressurization is restricted. Pressure values of 0.5, 0.6, 0.7, 0.8, 0.9 and 1 bar were selected for the initial stage of the investigation. In the second scenario, we determined the cavity pressure amplitudes corresponding to the

desired preload force values. The cavity was pressurized using these pressure values and the friction force was calculated with the desired preload force value. The reason for the two scenarios is because the preload value differs due to cavity pressure. Figure 15 illustrates the preload value due to different cavity pressures in these scenarios. The variation of the friction force amplitude with cavity pressure after contact in two simulations is shown in Figure 16. The friction force escalated with increasing cavity pressure, mimicking the results of the pressurized cavity before the contact.

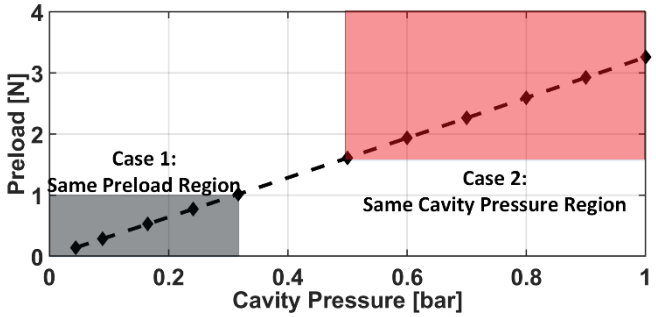

Figure 15. Variation of preload force value with the cavity pressure

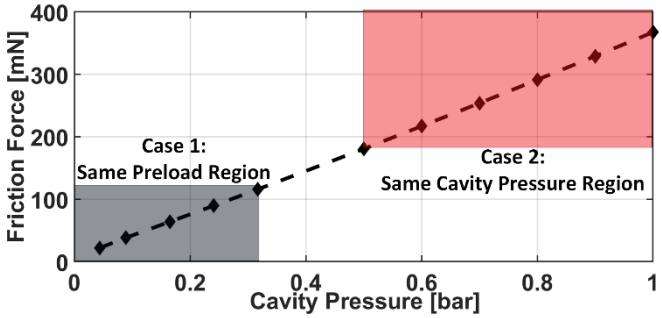

Figure 16. The effect of the cavity pressure on the friction force amplitude when the post is in contact with the counter surface

3.4. Adjusting the friction force by regulating cavity pressure

In the simulation studies conducted thus far, investigations have been made into the effects of the structural dimensions of the posts' cavities and cavity pressures on friction force amplitude. One aim of this study is to achieve an adjustable friction force between elastic posts and a flat and rigid body by regulating the post's cavity pressure. The variation in friction force amplitude is achieved by changing the cavity pressure of the post during full-slip motion and is shown in Figure 17, indicating the amplitude of the cavity pressure and its relationship with the friction force. The results demonstrate that the friction force adjusts almost linearly to the pressure change occurring during contact. The variation in the amplitude of friction force over time follows a similar pattern to the variation in cavity pressure over time. Therefore, the simulations have demonstrated that regulating cavity pressure can manipulate the amplitude of friction force.

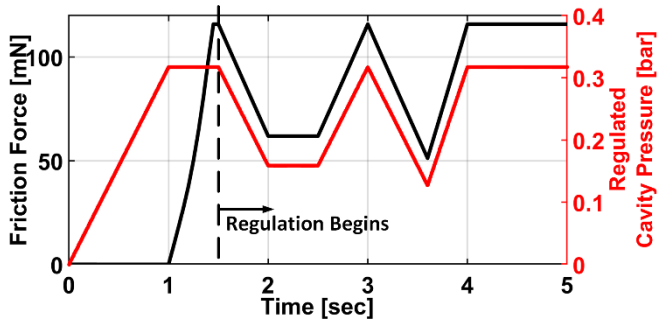

Figure 17. The effect of the cavity pressure on the friction force amplitude when the post is in contact with the counter surface

4. Conclusion

In this study, the friction dynamics of elastic cylindrical posts with cavity in contact with a flat, smooth, and rigid body were simulated in a finite-element based engineering program. The friction force amplitudes were calculated and the variation of the friction force with the structural parameters of the post cavity and the cavity pressure value of the post were obtained. The adjustable friction force by regulating the cavity pressure amplitude is shown in the simulations. The presence of a cavity reduces the friction force, with the cavity diameter having a greater influence on the reduction of the frictional force. Increasing the cavity pressure increases the friction force due to the increase in bending rigidity. Regulating the cavity pressure is shown to be an effective method of adjusting the friction force of an elastic post in contact with a rigid, smooth, flat surface.

Ethics committee approval and conflict of interest statement

This article does not require ethics committee approval. This article has no conflicts of interest with any individual or institution.

Acknowledgment

This work was supported by the Scientific and Technological Research Council of Turkey (TUBITAK) under grant no. 118M302.

References

[1] Wang, Z.W., Chen, M.W., Wu, J.W., Zheng, H.H., Zheng, X.F., 2010. A review of surface texture of tribological interfaces, In Applied Mechanics and Materials, Cilt. 37, s. 41-45. DOI: 10.4028/www.scientific.net/AMM.37-38.41

[2] Varenberg, M., Gorb, S. N., 2009. Hexagonal surface micropattern for dry and wet friction, Advanced Materials, Cilt. 21(4), s. 483–486. DOI: 10.1002/adma.200802734

[3] Etsion, I. 2004. Improving tribological performance of mechanical components by laser surface texturing, Tribology letters, Cilt. 17(4), s. 733–737. DOI: 10.1007/s11249-004-8081-1

[4] Etsion, I. 2005. State of the art in laser surface texturing, Journal of Tribology., Cilt. 127(1), s. 248–253. DOI: 10.1115/1.1828070

[5] Abdel-Aal, H. A. 2016. Functional surfaces for tribological applications: inspiration and design, Surface Topography: Metrology and Properties, Cilt. 4(4), s. 043001. DOI 10.1088/2051-672X/4/4/043001

[6] Mohd Nasir, F.F., Ghani, J.A., Zamri, W.F.H.W., Kasim S. M. 2019. State-of-the-art surface texturing and methods for tribological performance. World Review of Science, Technology and Sustainable Development, Cilt. 15, s. 330–357. DOI: 10.1504/WRSTSD.2019.104096

[7] Gachot, C., Rosenkranz, A., Hsu, S., Costa, H. 2017. A critical assessment of surface texturing for friction and wear improvement, Wear, Cilt..372, s. 21–41. DOI: 10.1016/j.wear.2016.11.020

[8] He, B., Chen, W., Wang, Q. J. 2008. Surface texture effect on friction of a microtextured poly (dimethylsiloxane)(PDMS), Tribology Letters, Cilt. 31(3), s. 187. DOI: 10.1007/s11249-008-9351-0

[9] Murarash, B., Itovich, Y., Varenberg, M. 2011. Tuning elastomer friction by hexagonal surface patterning, Soft Matter, Cilt. 7(12), s. 5553–5557. DOI: 10.1039/C1SM00015B

[10] Degrandi-Contraires, E., Poulard, C., Restagno, F., Léger, L. 2012. Sliding friction at soft micropatterned elastomer interfaces, Faraday discussions, Cilt. 156(1), s. 255–265. DOI: 10.1039/C2FD00121G

[11] Greiner, C., Merz, T., Braun, D., Codrignani, A., Magagnato, F. 2015. Optimum dimple diameter for friction reduction with laser surface texturing: the effect of velocity gradient, Surface Topography: Metrology and Properties, Cilt. 3(4), s. 044001. DOI: 10.1088/2051-672X/3/4/04400

[12] Greiner, C., Schäfer, M. 2015. Bio-inspired scale-like surface textures and their tribological properties, Bioinspiration & biomimetics, Cilt. 10(4), s. 044001. DOI: 10.1088/1748-3190/10/4/044001

[13] Greiner, C., Schafer, M., Popp, U., Gumbsch, P. 2014. Contact splitting and the effect of dimple depth on static friction of textured surfaces, ACS Applied Materials & Interfaces, Cilt. 6(11), s. 7986–7990. DOI: 10.1021/am500879m

[14] Eray, T., Sümer, B., Koc, I. M. 2016. Analytical and experimental analysis on frictional dynamics of a single elastomeric pillar, Tribology International, Cilt. 100, s. 293–305. DOI: 10.1016/j.triboint.2016.02.013

[15] Koc, I. M., Eray, T. 2018. Modeling frictional dynamics of a visco-elastic pillar rubbed on a smooth surface, Tribology International, Cilt. 127, s. 187-1999. DOI: 10.1016/j.triboint.2018.05.041

[16] Popov, V.L. 2013. Method of reduction of dimensionality in contact and friction mechanics: A linkage between micro and macro scales, Friction, Cilt. 1(1), s. 41–62. DOI: 10.1007/s40544-013-0005-3

[17] Marvi, H., Han, Y., Sitti, M. 2015. Actively controlled fibrillar friction surfaces, Applied Physics Letters, Cilt. 106(5), s. 051602. DOI: 10.1063/1.4907255

[18] Eray, T., Koç, I M., Sumer, B. 2019. Investigation of adhesion and friction of an isotropic composite pillar, Proceedings of the Institution of Mechanical Engineers, Part J: Journal of Engineering Tribology, Cilt. 233(4), s. 520-531. DOI: 10.1177/1350650118774427

[19] Tian, Y., Zhao, Z., Zaghi, G., Kim, Y., Zhang, D. and Maboudian, R. 2015. Tuning the friction characteristics of gecko-inspired polydimethylsiloxane micropillar arrays by embedding Fe3O4 and SiO2 particles, ACS Applied Material & Interfaces, Cilt. 7, s. 13232–13237. DOI: 10.1021/acsami.5b03301

[20] Fischer, S.C., Levy, O., Kroner, E., Hensel, R., Karp, J.M. and Arzt, E. 2016. Bioinspired polydimethylsiloxane-based composites with high shear resistance against wet tissue. journal of the mechanical behavior of biomedical materials, Cilt. 61, s. 87-95. DOI: 10.1016/j.jmbbm.2016.01.014

[21] Sharifi, S., Rux, C., Sparling, N., Wan, G., Mohammadi Nasab, A., Siddaiah, A., Menezes, P., Zhang, T. and Shan, W. 2021. Dynamically Tunable Friction via Subsurface Stiffness Modulation. Frontiers in Robotics and AI, Cilt. 8, s. 691789. DOI: 10.3389/frobt.2021.691789

[22] Arul, E.P., Ghatak, A. 2012. Control of adhesion via internally pressurized subsurface microchannels, Langmuir; Cilt. 28, s. 4339–4345. DOI: 10.1021/la204618u

[23] Prieto-López, L.O. and Williams, J.A., 2016. Using microfluidics to control soft adhesion. Journal of adhesion science and Technology, Cilt. 30(14), s. 1555-1573. DOI: 10.1080/01694243.2016.1155878

[24] Mohammadi Nasab, A., Luo, A., Sharifi, S., Turner, K.T. and Shan, W., 2020. Switchable adhesion via subsurface pressure modulation. ACS applied materials & interfaces, Cilt. 12(24), s .27717-27725. DOI: 10.1021/acsami.0c05367

[25] Eray, T., 2022. Tunable adhesion of an elastic pillar by pressurizing inner cavity, Proceedings of the Institution of Mechanical Engineers, Part J: Journal of Engineering Tribology, Cilt. 236(3), s. 541-551. DOI: 10.1177/13506501211018291

[26] Maugis, D., 2013. Contact, adhesion and rupture of elastic solids, 1st edition. Springer Berlin, Heidelberg, 414s.

[27] Carpick, R. W., Ogletree, D. F., Salmeron, M. 1997. Lateral stiffness: a new nanomechanical measurement for the determination of shear strengths with friction force microscopy, Applied Physics Letters, Cilt. 70(12), s. 1548-1550. DOI: 10.1063/1.118639